Solar RRL

RESEARCH ARTICLE OPEN ACCESS

SOLEY: A Package for Optical and Extended Detailed Balance Model for Photovoltaic Device Simulation

Zacharie Jehl Li-Kao[1,2]

[1]Electronic Engineering Department, Universitat Politècnica de Catalunya, Barcelona, Spain | [2]Barcelona Center for Multiscale Science & Engineering, Universitat Politècnica de Catalunya, Barcelona, Spain

Correspondence: Zacharie Jehl Li-Kao (zacharie.jehl@upc.edu)

Received: 6 May 2025 | **Revised:** 6 July 2025 | **Accepted:** 16 July 2025

Funding: Ayuda Ramon y Cajal Programme, Grant/Award Number: RYC2021-033239-I; EU-COST Action, Grant/Award Number: CA21148

Keywords: detailed balance | photovoltaic | simulation | solar cell modeling | transfer matrix method

ABSTRACT

SOLEY is a new photovoltaic device simulation package that combines the transfer matrix method for optical modeling with an extended detailed balance framework for electrical simulation. Unlike traditional drift-diffusion models, SOLEY operates with fewer input parameters while maintaining physical accuracy, and it is designed to be accessible for both research and educational purposes. The software includes several features such as native multijunction support, Schockley–Read–Hall recombination modeling with customizable pathways, batch calculation, optical stack optimization, and generation profile calculation. A validation of the model against solar cell capacitor simulator (SCAPS) demonstrates comparable results for a baseline kesterite solar cell. SOLEY is designed as a complementary tool to existing simulation software, offering rapid calculations suitable for high-throughput optimization and providing a perspective closer to thermodynamics on photovoltaic devices with a user-friendly interface. This freely distributed package is also the first one to rely mainly on an extension of the detailed balance model, and represents a counterpart to other photovoltaic modelling packages, which can be of interest for researchers of all levels of seniority.

1 | Introduction

Modeling is a cornerstone of the scientific method and can be used as a predictive tool, as an interpretation tool, or as a hypothesis-testing tool. This work pertains particularly to the modeling of photovoltaic devices, which over the past three decades has become a standard practice amongst the community, helped by several remarkable software developed by the community. One could cite solar cell capacitor simulator (SCAPS) [1, 2], the most widely used of those tools, combining a user-friendly graphical user interface (GUI) with robust defect physics and a broad range of valuable outputs. Other valuable software, such as Wx-AMPS [3], PC1D [4], AFORS-HET [5], Sesame [6], OghmaNano [7], and more recently SolCore [8] have each offered new modeling capabilities to experimentalists and theoreticians alike. It should be noted that while each package has its own advantages and drawbacks, they primarily rely on the drift-diffusion model, though a detailed balance model is sometimes also included to estimate the Shockley–Queisser limit of solar cells [8, 9]. The drift-diffusion model excels at simulating solar cells by solving coupled differential equations for carrier transport and electrostatics, and it provides a reliable modeling of device performance with moderate computational demands. However, it also demands an extensive knowledge of material parameters for each layer and interface in the stack, which can be challenging to obtain accurately often creates significant uncertainty in simulations. This is particularly true for emerging photovoltaic materials, where characteristics vary between laboratories and an exhaustive tabulation of parameters is lacking, which sometimes results in educated guesswork leading to unphysical results and conclusions being reported.

A more thermodynamic approach offers a possible alternative, as it conceptualizes the functioning of a solar cell as a balance of generation and loss currents and requires a lower set of input parameters to yield physical results. This approach, however, can remain sophisticated despite a seemingly more accessible framework; indeed, the thermodynamic formalism can be progressively enhanced to incorporate complex phenomena if experimental or theoretical inputs are available. And to the best of my knowledge, simulating software has aimed to use the detail balance framework to such an extent, often limiting the investigation to the Shockley–Queisser limit.

This work introduces the software SOLEY ('sun' in French West-Indies Creole) [10], which relies on a combining optical modeling by Transfer Matrix Method (TMM), and solar cell modeling using a detailed balance of generation and loss currents, with recombination being lumped into a recombination parameter J_0 as reported by Cuevas [11]. This latter parameter is a sum of currents comprising radiative and nonradiative losses, including a model of Shockley–Read–Hall (SRH) recombination recently reported in reference [12]. SOLEY is designed with accessibility in mind, including a GUI where each input is clearly identified. It is addressed to the broadest possible range of scientists with an interest in photovoltaics, from students to early career researchers to veterans of the field. It aims to be not only a valuable tool for research but also an educational tool to visualize the functioning of a solar cell. It incorporates functionalities which can be valuable to experimentalists, such as an optimization of the optical properties based on the material stack, but can also be a valuable tool for theoreticians and particularly density functional theory (DFT) specialists who wish to model new photovoltaic (PV) materials in a realistic architecture. It is also very fast and can be compatible with high-throughput simulation.

SOLEY also comes with limitations, some of which will be addressed in future updates and others are inherent to the chosen methodology, which will be detailed in this manuscript. It doesn't aim at replacing existing tools, which would be foolish and presumptuous considering their level of advancement, the duration of their development, and the number of talented researchers involved in their development. Rather, SOLEY should be viewed as a complement providing additional insights into the functioning of solar cells, the prediction of performance, and the interpretation of characterizations.

2 | Methodology and Functionalities

SOLEY possesses a GUI, which is illustrated Figure 1 and comprises two main elements.

The optical part is calculated using the Transfer Matrix Method (TMM), a comprehensive and widely used approach allowing for quantitative estimation of the optical profile of a material stack, particularly suited for the evaluation of thin film stacks. The device modeling uses the absorbance calculated for the selected PV absorbers of the stack to estimate the PV parameters and losses using an extension of the detailed balance formalism, which incorporates multiple recombination pathways, including defect-related recombination. This approach permits natively handling multiple absorbers in the structure, and SOLEY can

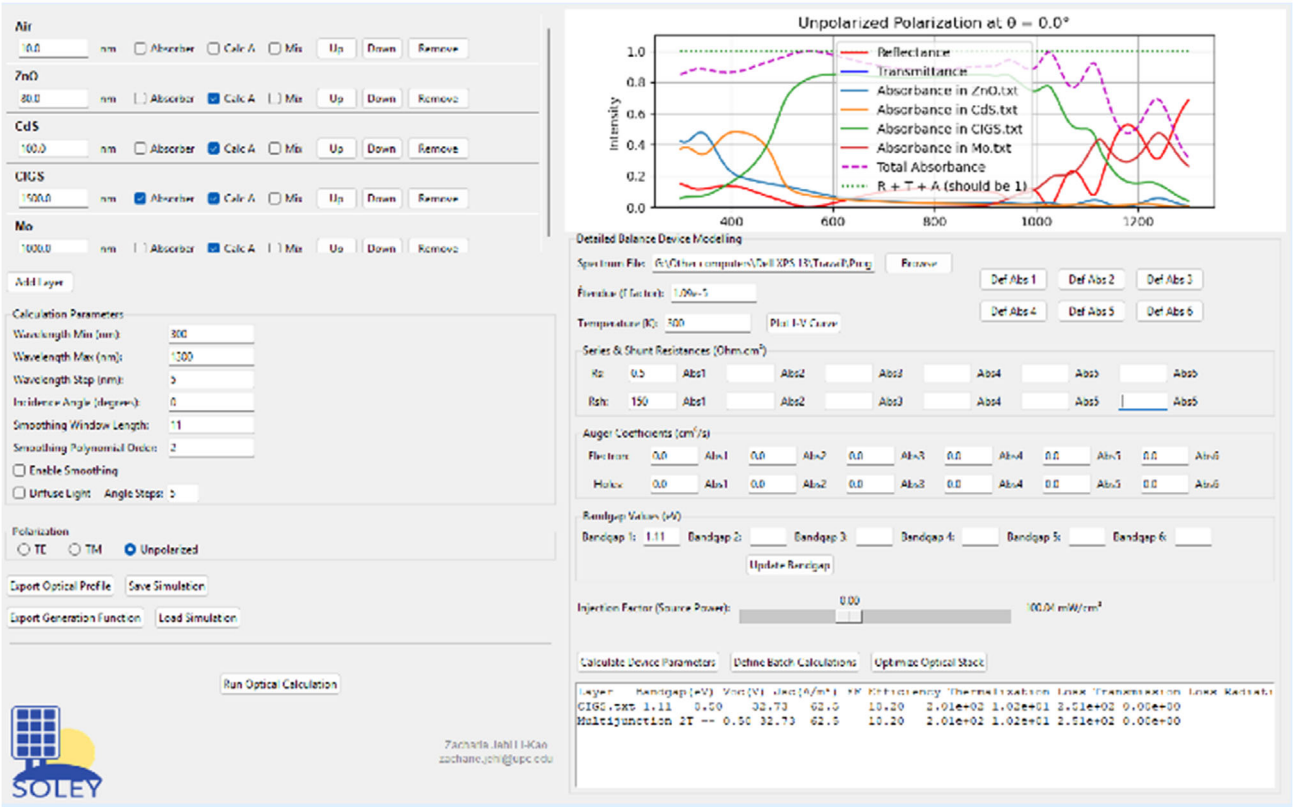

FIGURE 1 | GUI of SOLEY.

evaluate the multijunction performance (2-terminal) in a straightforward way at minimal computational cost.

2.1 | Optical Modelling

2.1.1 | General TMM Implementation

SOLEY implements the TMM to calculate the propagation of electromagnetic waves through multilayer stacks, accounting for reflection and transmission at each interface and propagation through each layer. The implementation is based on a tool previously developed and used in combination with SCAPS for evaluating the potential of thin film-based multijunctions in a more quantitative way [13, 14]. Light scattering effects are not implemented in the model at this point, though they are possible with the TMM [15]. The optical properties of each layer are defined by complex refractive indices (n + ik) as a function of the wavelength in nm, which are loaded from tabulated text files. For a multilayer stack with N layers, the system is defined by a total transfer matrix M that relates the electromagnetic field amplitudes at the initial and final boundaries:

$$\begin{pmatrix} E_0^+ \\ E_0^- \end{pmatrix} = M \begin{pmatrix} E_N^+ \\ E_N^- \end{pmatrix} \tag{1}$$

where $E_0^{+,-}$ are the forward and backward propagating electric field amplitudes in the incident medium, and $E_N^{+,-}$ are the forward and backward propagating electric field amplitudes in the exit medium.

This total transfer matrix is the product of interface matrices and propagation matrices:

$$M = D_0 \prod_{j=1}^{N-1} P_j D_j \tag{2}$$

where D_j is the interface matrix between layers j and $j+1$, and P_j is the propagation matrix through layer j. For each interface, the interface matrix is calculated using Fresnel coefficients r and t, which depend on the polarization state (transverse electric (TE) or transverse magnetic (TM)):

$$D_j = \frac{1}{t_j} \begin{pmatrix} 1 & r_j \\ r_j & 1 \end{pmatrix} \tag{3}$$

where $r_j = \frac{Q_j - Q_{j+1}}{Q_j + Q_{j+1}}$ and $t_j = \frac{2Q_j}{Q_j + Q_{j+1}}$ are the reflection and transmission coefficients. For TE polarization, $Q_j = k_{x,j}$, while for TM polarization, $Q_j = \frac{k_{x,j}}{n_j^2}$, where $k_{x,j}$ is the wave vector component perpendicular to the interfaces.

The propagation matrix considers the phase accumulation as light travels through a layer:

$$P_j = \begin{pmatrix} e^{-ik_{x,j}d_j} & 0 \\ 0 & e^{ik_{x,j}d_j} \end{pmatrix} \tag{4}$$

where d_j is the thickness of layer j.

Therefore, from the total system matrix, the reflection and transmission coefficients are calculated as $r = \frac{M_{10}}{M_{00}}$ and $t = \frac{1}{M_{00}}$.

The reflectance (R) and transmittance (T) are then calculated in the appropriate polarization state. It should be highlighted that when defining a material stack in SOLEY, it is essential that the first and last layers are defined as air (or another ambient medium) as the TMM requires well-defined boundary conditions.

2.1.2 | Absorption and Generation Profile Calculation

SOLEY calculates absorption within each layer using the Poynting vector approach. For a selected layer of interest, the electromagnetic fields are calculated at the entrance and exit boundaries, and the difference in the Poynting vector component along the axis of propagation gives the absorbance A:

$$A = \frac{S_{\text{in}} - S_{\text{out}}}{S_{\text{inc}}} \tag{5}$$

where S_{in} and S_{out} are the Poynting vectors at the entrance and exit of the layer, and S_{inc} is the incident Poynting vector on the stack.

To calculate the spatially resolved generation function within the absorber layers, SOLEY calculates the local electric field at each position within the layer and calculates the local generation rate using the formula:

$$G(x) = \int \frac{\alpha(\lambda).I_{\text{local}}(x,\lambda).I_0(\lambda)}{h\upsilon} d\lambda \tag{6}$$

where:

- $\alpha(\lambda) = \frac{4\pi k(\lambda)}{\lambda}$ is the absorption coefficient
- $I_{\text{local}}(x,\lambda)$ is the local field intensity
- $I_0(\lambda)$ is the incident spectral intensity
- $h\upsilon$ is the photon energy

This integration is performed over the incident spectrum, which results in the generation rate in units of photons/m³/s at each position within the layer. This generation function is particularly valuable for device simulations and can be exported to other software such as SCAPS.

Finally, as different incident angles can be considered, SOLEY permits the simulation of the optical profile under diffuse light by integrating over those different angles. This can be particularly valuable for indoor photovoltaics, which is being increasingly discussed in the PV community.

2.1.3 | Numerical Stability Enhancements

The implementation of the TMM in SOLEY includes several numerical stability enhancements to ensure reliable calculations across a wide range of wavelengths and material combinations. Without these enhancements, conventional TMM

implementations can suffer from numerical overflow or underflow, particularly when dealing with highly absorbing or thick layers.

Key stability features include an adaptive matrix conditioning based on condition number monitoring, a matrix normalization to prevent overflow in highly absorbing systems, an enhanced propagation matrix calculation using logarithmic techniques for thick absorbing layers, and a regularized field coefficient calculation to handle near-singular matrices. These enhancements allow for robust performance even for complex multilayer stacks with high contrast in optical properties. Stacks of more than 30 layers have been tested without yielding unphysical results. Additionally, thick absorbing layers such as crystalline silicon can also be modeled with reasonable accuracy, which can be challenging with the TMM. However, there are still limitations even with those optimizations, and if the model is pushed far enough (for instance, 300 μm thick c-Si with a back Ag reflector), small divergences may still be observed. But for standard solar cell architectures, the model remains resilient enough to be used.

2.1.4 | Limitations of the Model

Whilst the TMM implementation in SOLEY is used for many applications, it has certain limitations:

- **Coherent light only**: The current implementation assumes coherent light propagation, which is appropriate for thin films but leads to unrealistic interference patterns in thick transparent substrates like glass. These interference patterns should be washed out due to factors like substrate thickness variations, beam divergence, and finite spectral resolution. This is a common limitation of the TMM, and while implementing noncoherent calculations such as Beer–Lambert lead to smoother curves, those are not physical ($R+T+A\neq 1$). As a backup solution, a smoothing option is present in SOLEY.
- **No light scattering**: The model does not account for light scattering at rough interfaces, and therefore no light trapping unlike in many real devices.
- **Complex optical behaviour**: More advanced light trapping structures such as Fabry-Perot resonance [16] are ignored, and other approaches, such as rigorous coupled-wave analysis (RCWA) would be much more suited [17].

Future developments of SOLEY will address some of these limitations, with a priority to implement an incoherent calculation mode for thick substrates. However, for typical thin-film solar cell applications where the active layers are in the nanometer to micrometer range, the current implementation provides excellent accuracy for predicting optical behavior and generation profiles.

2.2 | Device Modelling

2.2.1 | Detailed Balance Framework

SOLEY implements a detailed balance approach for device modelling, which conceptualizes the solar cell operation as a balance between generation currents and various recombination loss mechanisms. This can be viewed as an extension of the Shockley–Queisser limit [18]. This thermodynamic framework allows for the prediction of fundamental device parameters whilst requiring fewer input parameters than drift-diffusion models.

The base implementation calculates the short-circuit current density by integrating the product of the spectral photon flux and the absorber's quantum efficiency (derived from the optical absorption calculation). Subsequently, the open-circuit voltage, fill factor, and efficiency are determined by balancing this generation current against various recombination mechanisms.

The model accounts for several fundamental loss mechanisms:

1. Radiative recombination: The unavoidable thermodynamically required recombination current is obtained from the detailed balance principle and calculated as:

$$J_{0,rad} = q\int_{E_g}^{\infty} \frac{2\pi E^2}{h^3c^2}\frac{1}{\exp\left(\frac{E}{kT}\right)-1}dE \tag{7}$$

where E_g is the bandgap energy in eV (converted to joules for integration), q is the elemental charge in Coulomb, k is the Boltzmann constant in $J.K^{-1}$, T is the temperature in K, h is Planck's constant J.s, and c is the speed of light in vacuum in $m.s^{-1}$ This formulation corresponds to the rigorous integration of the black-body photon density of states above the bandgap and does not require the étendue factor f used in the approximate closed-form expression.

2. Thermalization losses: Energy lost when carriers relax to band edges, which is calculated as:

$$P_{\text{therm}} = \int_{E_g}^{\infty} P_{\text{inc}}(E)\frac{E-E_g}{E}dE \tag{8}$$

where P_{inc} is the incident spectral power density in $W.m^{-2}.eV^{-1}$.

3. Transmission losses: Photons with energy below the bandgap that are not absorbed:

$$P_{\text{trans}} = \int_{0}^{E_g} P_{\text{inc}}(E)dE \tag{9}$$

4. Auger recombination: This nonradiative three-particle process is approximated with temperature and bandgap dependence:

$$C_{n,p}(T,E_g) = C_{A0}\left(\frac{T}{300}\right)^{\alpha} exp\left(-\frac{E_g}{3kT}\right) \tag{10}$$

And for a p-type absorber:

$$J_{0,\text{Auger}} = q.d.C_p.N_a^2.n_i \tag{11}$$

where C_{A0} is the Auger coefficient, d is the absorber thickness, N_a is the doping concentration, and n_i is the intrinsic carrier concentration, which is calculated using the standard semiconductor physics approach based on effective densities of states and bandgap. More details are given in the manual of SOLEY.

2.2.2 | SRH Recombination Model

The SRH recombination model in SOLEY goes beyond simplified approaches by providing a physically-grounded calculation of recombination through defect states. The SRH saturation current density is modeled as:

$$J_0^{SRH} = J_{00} exp\left(- \frac{E_a}{nkT} \right) \tag{12}$$

where E_a is the activation energy, n is the ideality factor, and J_{00} is a prefactor with two components:

$$J_{00} = J_{00}^{\text{bulk}} + J_{00}^{\text{interface}} \tag{13}$$

For the bulk and interface recombination, respectively. The explicit derivation of both factors is given in reference [12]. Both factors can either be experimentally fitted through temperature dependent current–voltage analysis or calculated via parameters which can be obtained through DFT calculation. SOLEY permits to either calculate the prefactors or to directly input them in case of fitting, which offers flexibility for both experimentalists and theoreticians. Limiting SRH recombination to interface and bulk currents is justified by the fact that dominant defects will act as bottlenecks to the performance.

2.2.3 | Custom Recombination Pathways

However, this can be limiting in some cases. Therefore, one of SOLEY's features is the ability to define custom recombination pathways through a user-defined J_0^{custom} function. This capability greatly extends the applicability of the model beyond standard p–n junctions. Users can input arbitrary expressions for recombination currents that capture phenomena not explicitly included in the built-in models. For example, users can define voltage-dependent back-interface recombination with:

$$J_0^{\text{custom}}(V) = J_{00}^{\text{back}} exp\left(\frac{qV}{n_{\text{back}} kT} \right) \tag{14}$$

Other examples include modelling grain boundary recombination, tunnel-assisted recombination, or interface recombination at heterojunctions with complex band alignments. The model is, however, not suitable for advanced concepts that rely fundamentally on nonequilibrium carrier distributions or quantum effects, such as hot carrier solar cells, intermediate band devices, or quantum dot solar cells.

2.2.4 | Model Limitations

Despite its flexibility, the detailed balance approach implemented in SOLEY has several important limitations that users should be aware of. First, there is no explicit transport modelling. Unlike drift-diffusion models, SOLEY does not solve the transport equations directly, which means it cannot capture effects like carrier collection issues due to poor mobility or low diffusion lengths. These effects must be implicitly included through the recombination parameters J_0. Also, while the p–n interface and band alignment are considered in $J_{00}^{\text{interface}}$, the model does not calculate or use the full band diagram. This simplification means that effects like barrier-limited transport, band bending, and space charge regions are not explicitly modeled. The model also assumes homogeneous material properties throughout each layer, which means that spatial variations due to grading, defect distribution, or local structural differences are not considered. Tools such as SCAPS are much better suited for such an investigation. Similarly, the model simplifies the interactions at contacts, which can be inadequate for devices where contact selectivity, work function alignment, or interface dipoles play critical roles. And finally, SOLEY performs as a fully steady-state analysis, which means that it cannot capture transient phenomena that might be important for some device characterization methods or operational conditions.

For applications where these limitations are significant, traditional drift-diffusion modelling tools would be more appropriate. However, for many practical cases, particularly in early-stage device design and material exploration, SOLEY's approach may provide valuable insights with significantly reduced computational complexity and input parameter requirements. As always, it is up to the user to understand the limitations of the tools when using them.

2.2.5 | Additional Functionalities

SOLEY incorporates several additional functionalities that enhance its utility for device optimisation and analysis. Some of these features are implemented to extend the physical modeling capabilities, but others are just designed to improve usability and facilitate high-throughput parameter scans. The illumination intensity from well below 1-sun (useful for indoor PV application, for example) to high concentration (up to 46,300 suns) can be varied via an injection slider. It should be noted that nonlinearities appearing at high concentration are currently not considered in SOLEY, and such values should be used for idealized case studies only, at the user's discretion. Also, SOLEY has an optical stack optimization module that can systematically vary the thicknesses of selected layers within a specified range to maximize device efficiency, including for multijunction evaluation (up to 6 subcells can be defined). This functionality uses a two-stage optimization approach: an initial grid search followed by an optional refinement stage for higher accuracy. The optimization considers the interplay between optical absorption and electrical performance, making it an interesting tool for early device structure engineering. As previously mentioned, SOLEY offers the possibility to export spatially-resolved generation profiles, which can serve as input for device simulations in other software.

While light scattering from rough surfaces is not implemented yet, SOLEY proposes the possibility to mix the optical properties of two consecutive layers by using the Bruggeman equation for effective medium approximation. This is particularly useful to simulate porous layers and antireflective coatings (ARC) and can be a decent approximation to pyramidal-shaped interfaces when light scattering is not a dominant factor. Finally, Soley integrates an automated algorithm to determine the bandgap from the absorption profile using a Gaussian fitting approach on the first derivative of the absorption curve; while it provides a consistent method for bandgap extraction from optical data, it can be occasionally unreliable, and the user has the possibility

to input directly a bandgap value. Beyond their application in the context of scientific research, these additional features can be valuable tools for educational purposes, such as showing directly the impact of shunt/series resistance as a function of carrier injection.

3 | Useability demonstration

3.1 | Native Multijunction Support

Evaluating multijunction solar cells with SOLEY is easy and reliable, as illustrated in this paragraph. Indeed, as the complete optical profile can be evaluated through the TMM, SOLEY simply performs a detailed balance calculation on layers selected as absorbers, including all the user-defined bottlenecks (resistance, Auger recombination, SRH recombination). SOLEY calculates the PV parameters of each subcell (up to 6 can be defined), and computes the performance of the multijunction in a 2 Terminal configuration by matching to the subcell's lowest current, adding the V_{oc} of each subcell, and determining the fill factor (FF) from the JV curve directly.

An illustration is provided Figure 2 where an ideal kesterite CZTS/CZTSe tandem is modeled. For simplification purposes, no SRH recombination is defined, Auger recombination is ignored, and the series and shunt resistance are assumed to be 0 and infinite, respectively. The baseline stack is unoptimized on purpose, with a poor current matching between the top CZTS and the bottom CZTSe, which results in a comparatively lower tandem FF and a 2T tandem efficiency only marginally higher than that of the top cell, at 67% and 24.9% respectively, despite the very high FF of individual subcells (>80%), as seen in both the JV curves and the table Figure 2. This lack of optimization permits to introduce a possibly useful functionality of SOLEY, which allows to run a batch of calculations using a user-defined thickness range and number of steps for selected layers of the stack, and searches for the optimum combination in terms of efficiency. The usefulness of this feature is illustrated Figure 2a,c, where the stack is optimized according to the conditions shown in the enclosed table. While there is still a significant reflectivity in the red and near IR region, and the material stack ought to be optimized further with a broader band ARC, SOLEY does find the optimum conditions within the defined parameters. The 'optimized' PV performance is reported in Figure 2. This functionality can be useful not only for optimizing multijunction stacks, but also to optimize ARCs or transparent conductive oxide (TCOs') thickness and maximize absorption in the layers of interest. While for now, a brute-force approach to optimisation is used, which can take a while for complex stacks where 3 or more layers are simultaneously optimized, this will be refined with more complex algorithms and parallel computing in future versions of SOLEY.

3.2 | Influence of SRH Recombination

As mentioned in the methodology section, SOLEY relies on two main processes, summarized by (Equation 12) and (13), to calculate the SRH recombination current J_0^{SRH}. Indeed, the

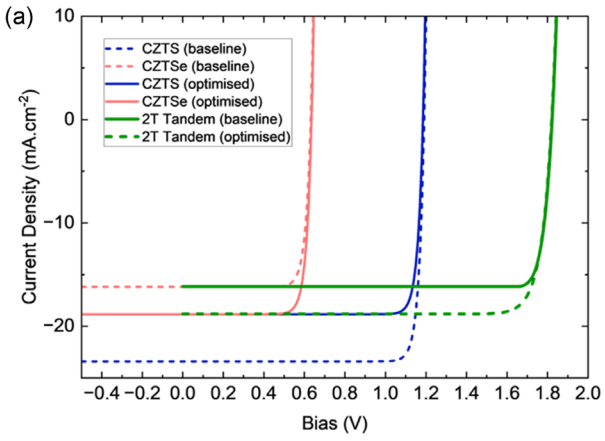

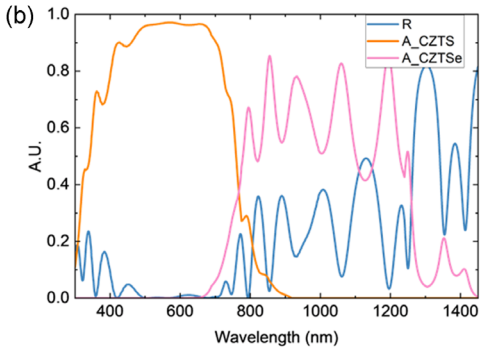

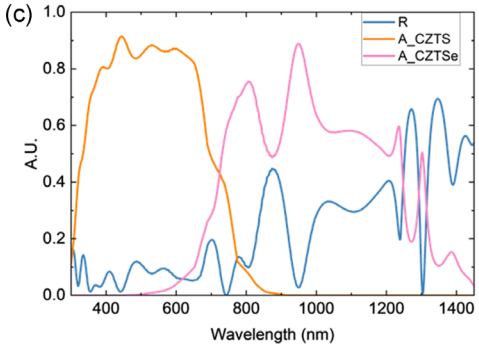

Baseline: Air/**MgF_2(100nm)**/ITO/ZnS/**CZTS(1500nm)**/ITO/CdS/**CZTSe(1500nm)**/Mo/Air

Optimised: Air/**MgF_2(150nm)**/ITO/ZnS/**CZTS(800nm)**/ITO/CdS/**CZTSe(2300nm)**/Mo/Air

	Layer	Bandgap(eV)	Voc(V)	Jsc(A/m^2)	FF (%)	PCE (%)
Baseline	CZTS	1.55	1.19	23.4	89.7	24.99
	CZTSe	1	0.63	16.19	83.4	8.52
	Multijunction2T	--	1.82	16.19	91.8	25.81
Optimised Optics	CZTS	1.55	1.19	18.85	89.7	20.02
	CZTSe	1	0.64	18.85	83.4	9.99
	Multijunction2T	--	1.82	18.85	87.5	29.97

FIGURE 2 | (a) JV curves for a CZTS/CZTSe tandem solar cell. Dashed curves: nonoptimized optical stack. Solid lines: optimised optical stack. (b) simulated optical profile of the full kesterite tandem solar cell used as baseline. (c) simulated optical profile of the full kesterite tandem solar cell optimized for current matching between CZTS and CZTSe.

assumption is made that only the dominant bulk and interface recombination processes influence the performance, and one is given the possibility to either directly input the J_{00}^{bulk} and $J_{00}^{interface}$. To illustrate the functioning of this feature, we reprise the 'optimized' stack from Figure 2 and implement parameters inspired by those reported by Scaffidi et al. [12]. The complete set of parameters used to calculate the J_0^{SRH} is reported Table **1**. Additionally, realistic series and shunt resistances of 2 and 5000 $\Omega.cm^2$ are used for both subcells. The resulting performance is shown Figure 3. As can be seen, both V_{oc} and FF are largely affected while the J_{sc} remains mostly unchanged, which is expected for a J_0^{SRH} within that range. The overall performance is within the range of excellent state-of-the-art Kesterite solar cells, and generally consistent with our previous work on the tandem Kesterite modeled by SCAPS [14].

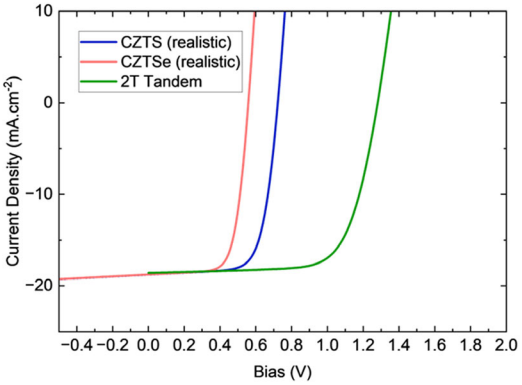

	Layer	Bandgap(eV)	Voc(V)	Jsc(A/m²)	FF (%)	PCE (%)
"Realistic" Kesterite Tandem	CZTS	1.55	0.723	18.81	71.3	9.69
	CZTSe	1	0.558	18.45	70.7	7.27
	Multijunction2T	--	1.281	18.45	71.3	16.83

FIGURE 3 | JV curve and PV parameters for a Kesterite tandem solar cell using realistic input parameters as reference Table 1.

3.3 | Custom SRH Recombination

The two included recombination processessare inspired by the work from Scaffidi et al. on thin film Kesterite solar cells [12]. It would remain to be verified if such an approach remains valid across a broad range of PV technologies, including Perovskite and crystalline Silicon.

Nonetheless, this cannot, in some cases, fully account for the physics of recombination in a solar cell. To avoid limiting the user, an input box is located in the recombination definition panel, where arbitrary functions can be defined using the Python formalism (PEMDAS) and a set of listed parameters. This is particularly valuable for recombination, which depends on the voltage, and can simulate the effect of a double/reverse diode. In thin film technologies, it can also be used to account for back contact recombination becoming prevalent for ultra-thin films [19], which is particularly relevant for emerging antimony chalcogenides as their extremely high absorption permits to fabricate solar cells with an absorber thickness ofs 50–100 nm. Future updates of SOLEY will hard-code additional common recombination processes based on the literature and on user feedback, but in the meantime, the presence of this input box allows to easily customize recombination processes to match reality.

TABLE 1 | Input parameters used for the modeling of SRH recombination in a Kesterite tandem solar cell.

	Parameter Name	CZTS	CZTSe
User-defined	Temperature [K]	300	300
	Activation Energy Ea [eV]	1.3	1
	Ideality Factor [n]	1.7	1.3
	Conduction Band DOS (Absorber) Nc_abs [cm^{-3}]	1.00E + 18	1.00E + 18
	Valence Band DOS (Absorber) Nv_abs [cm^{-3}]	1.00E + 18	1.00E + 18
	Permittivity (Absorber) epsilon_abs [F/m]	8.00E-11	8.00E-11
	Built-in Voltage Vbi [V]	0.6	0.4
	Absorber Doping Concentration Na [cm^{-3}]	1.00E + 15	1.00E + 15
	Thermal Velocity vth [cm/s]	1.00E + 07	1.00E + 07
	Capture Cross section (Bulk) sigma_n [cm^2]	1.00E-13	1.00E-13
	Trap Density (Bulk) Nt_bulk [cm^{-3}]	1.00E + 15	1.00E + 15
	Surface Recombination Velocity Sp [cm/s]	1.00E + 04	1.00E + 04
	Conduction Band DOS (Buffer) Nc_buff [cm^{-3}]	2.00E + 18	2.00E + 18
	Valence Band DOS (Buffer) Nd_buff [cm^{-3}]	1.00E + 16	1.00E + 16
	Interface Parameter theta	0.3	0.3
Calculated	**Bulk SRH Prefactor J00_bulk [mA/cm^2]**	**8.39E + 05**	**1.03E + 06**
	Interface SRH Prefactor J00_interface [mA/cm^2]	**8.23E + 06**	**8.23E + 06**
	SRH recombination current J0_SRH [mA/cm^2]	**1.29E-06**	**1.10E-06**

4 | Use Case: Comparison with SCAPS and Experiments on a Realistic CZTSe Baseline

SCAPS from Gent University [1, 2] has been widely recognised by the PV community as a reliable and user-friendly simulation package for solar cells, which has grown over the years to become a highly functional tool incorporating advanced device physics. Being based on the drift diffusion model, and not incorporating optical modelling or multijunction natively, its philosophy and use cases often, but not always, differ from SOLEY. Nonetheless, SCAPS is a reliable benchmark to assess the logic of SOLEY by using the simple case of a reference thin-film solar cell. In a previous work on Kesterite solar cells [14], we proposed a SCAPS baseline for modeling CZTSe solar cells, which was based on an extensive set of materials and device characterization, and accurately represented our reference experimental solar cell. This baseline includes both bulk and interface defect states, which makes it an ideal candidate for a one-to-one comparison between SOLEY, SCAPS, and a reference experimental cell. The objective is twofold:

- Showing that SOLEY yields credible results by using SCAPS and experiments as a benchmark.
- Illustrating how two completely different sets of equations will, as they should, yield a very similar result as long as the proper equations for each recombination process (including SRH) are known.

To ensure that both models operate with an identical optical basis, the front-surface reflectivity calculated by SOLEY was used as input in SCAPS. A more integrated approach, such as importing the full generation profile computed by SOLEY into SCAPS, as demonstrated by the group of J.-F. Guillemoles with OptiSCAPS [20], could also be used in future work.

All material and electrical parameters are kept consistent between the two simulations. In SOLEY, the activation energy $Ea = 0.95\,eV$ and ideality factor $n = 1.42$ were adjusted using the batch and optimize functionalities, as these are not explicit inputs in SCAPS and must be extracted phenomenologically, in each case with the goal of approaching the experimental result. The values obtained for both Ea and n are within the expected range for this class of solar cell.

The resulting JV curve obtained with both packages is presented Figure 4. An excellent agreement in terms of figure of merits and general shape of the curves is obtained, with values within less than 1% between both packages, except for the FF (66.3% experimentally, 66.0% in SOLEY, and 67.9% in SCAPS). This close match reinforces the idea that, despite relying on fundamentally different formalisms, the thermodynamic in SOLEY and the electrodynamic in SCAPS, both models accurately describe the same physical device and both are equally consistent with experimental observation. Beyond its benchmarking value, this comparison also has an educational merit: it illustrates that the thermodynamic approach is not limited to ideal cases such as the Shockley–Queisser limit, but can also reproduce realistic device behavior when appropriate recombination models, such as SRH, are included. Users are encouraged to explore such comparisons

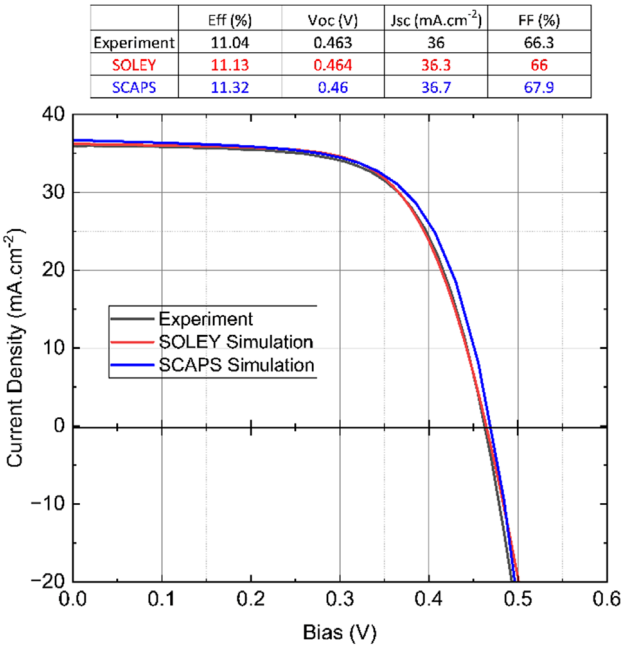

FIGURE 4 | JV comparison of the Kesterite baseline from reference [14] for an experimental sample, the SCAPS model and the SOLEY model.

to deepen their understanding of the underlying physics and appreciate the complementary strengths of both modelling approaches. As SOLEY continues to evolve and support more recombination mechanisms, more advanced comparisons will become straightforward, though even now, the built-in custom recombination function allows reproducing most cases of practical interest.

5 | Conclusion

SOLEY is a new photovoltaic device simulation package that combines the TMM and an extended detailed balance model to accurately reproduce the behavior of photodiodes under illumination. The chosen framework offers several advantages, as well as limitations, compared to the drift-diffusion model used in the vast majority of other solar cell simulation software. SOLEY can operate with a more limited set of input parameters. The celerity at which detailed balance calculations are done also permits high-throughput batch calculations useful to brute-force optimizations, which can be more reliable than fitting to avoid converging toward unphysical values. SOLEY includes several useful functionalities, amongst which the possibility to use direct or diffuse illumination (valuable for applications such as indoor PV), layer stack optical optimisation, mixed optical indices materials, native support of multijunction architectures, and generation function calculation. The optical algorithm, while primarily designed for thin films, includes many stability checks which permit to simulate thick absorbing layers and accurately simulate crystalline silicon solar cells. It should be stressed that SOLEY's aim is to complement existing drift-diffusion simulation tools, and certainly not to replace them.

For those reasons, SOLEY differentiates itself from other photovoltaic simulation packages, and its GUI makes it accessible to a

wide audience within the research community, as well as a possibly valuable educational tool. SOLEY will be updated by me and hopefully others through the upcoming years. SOLEY is available at Reference [10].

Acknowledgments

Z.J.L.K. thanks the Spanish Ministry of Science and Innovation for the financial support in the frame of the Ayuda Ramon y Cajal Programme (grant no. RYC2021-033239-I) and EU-COST Action (grant no. CA21148).

Conflicts of Interest

The author declares no conflicts of interest.

Data Availability Statement

The data that support the findings of this study are openly available in Zenodo at https://zenodo.org/records/16151991, reference number 16151991.

References

1. M. Burgelman, P. Nollet, and S. Degrave, "Modelling Polycrystalline Semiconductor Solar Cells," *Thin Solid Films* 361-362 (2000): 527–532.

2. M. Burgelman, K. Decock, S. Khelifi, and A. Abass, "Advanced Electrical Simulation of Thin Film Solar Cells," *Thin Solid Films* 535 (2013): 296–301.

3. Y. Liu, M. Ahmadpour, J. Adam, J. Kjelstrup-Hansen, H.-G. Rubahn, and M. Madsen, "Modeling Multijunction Solar Cells by Nonlocal Tunneling and Subcell Analysis," *IEEE Journal of Photovoltaics* 8, no. 5 (2018): 1363–1369.

4. D. A. Clugston and P. A. Basore, "*PC1D Version 5: 32-Bit Solar Cell Modeling on Personal Computers*," in Conference Record of the Twenty Sixth IEEE Photovoltaic Specialists Conference-1997, (IEEE, 1997), 207–210.

5. R. Varache, C. Leendertz, M. E. Gueunier-Farret, J. Haschke, D. Muñoz, and L. Korte, "Investigation of Selective Junctions Using a Newly Developed Tunnel Current Model for Solar Cell Applications," *Solar Energy Materials and Solar Cells* 141 (2015): 14–23.

6. B. Gaury, Y. Sun, P. Bermel, and P. M. Haney, "Sesame: A 2-Dimensional Solar Cell Modeling Tool," *Solar Energy Materials and Solar Cells* 198 (2019): 53–62.

7. R. C. I. MacKenzie, T. Kirchartz, G. F. A. Dibb, and J. Nelson, "Modeling Nongeminate Recombination in P3HT: PCBM Solar Cells," *The Journal of Physical Chemistry C* 115, no. 19 (2011): 9806–9813.

8. D. Alonso-Álvarez, T. Wilson, P. Pearce, M. Führer, D. Farrell, and N. Ekins-Daukes, "Solcore: A Multi-Scale, Python-Based Library for Modelling Solar Cells and Semiconductor Materials," *Journal of Computational Electronics* 17, no. 3 (2018): 1099–1123.

9. W. Shockley and H. J. Queisser, "Detailed Balance Limit of Efficiency of p-n Junction Solar Cells," *Journal of Applied Physics* 32, no. 3 (1961): 510–519.

10. Zacharie Jehlli-kao (Zenodo, 2025), https://zenodo.org/records/16151991.

11. A. Cuevas, "The Recombination Parameter J0," *Energy Procedia* 55 (2014): 53–62.

12. R. Scaffidi, A. Jimenez-Arguijo, Y. Gong, et al., "Temperature- and Light-Intensity-Dependent Current–voltage Analysis Applied to High-Efficiency Solution-Processed Kesterite Solar Cells," *Newton* 916 (2024): 100198.

13. K. J. Tiwari, Giraldo S., M. Placidi, et al., "Feasibility of a Full Chalcopyrite Tandem Solar Cell: A Quantitative Numerical Approach," *Solar RRL* 5, no. 7 (2021): 2100202.

14. A. Jimenez-Arguijo, et al., "Setting the Baseline for the Modelling of Kesterite Solar Cells: The Case Study of Tandem Application," *Solar Energy Materials and Solar Cells*, 251 (2023): 112109.

15. D. Cozza, et al., "Optical Modeling and Optimizations of Cu 2 ZnSnSe 4 Solar Cells Using the Modified Transfer Matrix Method," *Optics Express* 24, no. 18 (2016): A1201–A1209.

16. B. Behaghel, Tamaki R., N. Vandamme, et al., "*Absorption Enhancement through Fabry-Pérot Resonant Modes in a 430 nm Thick InGaAs/GaAsP Multiple Quantum Wells Solar Cell*," *Applied Physics Letters* 106, no. 8 (2015): 081107, https://doi.org/10.1063/1.4913469.

17. J. P. Hugonin and P. Lalanne, "*RETICOLO Software for Grating Analysis*," arXiv: arXiv:2101.00901 (2025), https://doi.org/10.48550/arXiv.2101.00901.

18. J.-F. Guillemoles, T. Kirchartz, D. Cahen, and U. Rau, "Guide for the Perplexed to the Shockley–Queisser Model for Solar Cells," *Nature Photonics* 13, no. 8 (2019): 501–505.

19. J. Z. Li-Kao, N. Naghavi, F. Erfurth, et al., "Towards Ultrathin Copper Indium Gallium Diselenide Solar Cells: Proof of Concept Study by Chemical Etching and Gold Back Contact Engineering," *Progress in Photovoltaics: Research and Applications* 20, no. 5 (2012): 582–587.

20. L. Lombez, M. Soro, A. Delamarre, et al., "Revisiting the Interpretation of Biased Luminescence: Effects on Cu(In, Ga)Se2 Photovoltaic Heterostructures," *Journal of Applied Physics* 116, no. 6 (2014): 064504, https://doi.org/10.1063/1.4891525.

Supporting Information

Additional supporting information can be found online in the Supporting Information section. **Figure S1**. Comparison between the optical modelling by SOLEY and by RefDex. **Figure S2**. Comparison between SCAPS and SOLEY using parameters from the baseline definition of a CIGSe solar cell "Example CIGS.def".